Front. Earth Sci. 2013, 7(1): 103–111
DOI 10.1007/s11707-012-0346-7

RESEARCH ARTICLE

An artificial neural network approach to estimate evapotranspiration from remote sensing and AmeriFlux data

Zhuoqi CHEN[1], Runhe SHI (✉)[2], Shupeng Zhang[1]

1 College of Global Change and Earth System Science, Beijing Normal University, Beijing 100875, China
2 Key Laboratory of Geographic Information Science, East China Normal University, Shanghai 200062, China

Abstract A simple and accurate method to estimate evapotranspiration (ET) is essential for dynamic monitoring of the Earth system at a large scale. In this paper, we developed an artificial neural network (ANN) model forced by remote sensing and AmeriFlux data to estimate ET. First, the ANN was trained with ET measurements made at 13 AmeriFlux sites and land surface products derived from satellite remotely sensed data (normalized difference vegetation index, land surface temperature and surface net radiation) for the period 2002–2006. ET estimated with the ANN was then validated by ET observed at five AmeriFlux sites during the same period. The validation sites covered five different vegetation types and were not involved in the ANN training. The coefficient of determination (R^2) value for comparison between estimated and measured ET was 0.77, the root-mean-square error was 0.62 mm/d, and the mean residual was −0.28. The simple model developed in this paper captured the seasonal and interannual variation features of ET on the whole. However, the accuracy of estimated ET depended on the vegetation types, among which estimated ET showed the best result for deciduous broadleaf forest compared to the other four vegetation types.

Keywords AmeriFlux, artificial neural network (ANN), evapotranspiration (ET), remote sensing

1 Introduction

Evapotranspiration (ET), the combination of evaporation from soil and transpiration from plants, is a critical component of the energy budget and water cycle. Land ET returns about 60% of land precipitation to the atmosphere (Oki and Kanae, 2006). Thus, an accurate estimation of ET will greatly improve the monitoring of changes in the water cycle, which is an important part of on-going global climate change (Jung et al., 2010). Although there are many ground sites at which accurate ET observations are made, these sites are sparsely distributed and their ET observations do not represent the regional ET condition. It is therefore unrealistic to estimate regional and even global ET from these ground observations alone. Satellite remote sensing could provide large-area observations of the land surface frequently and continuously, and it is thus regarded as the most feasible approach to obtaining a regional estimation of ET. Therefore, developing a remote sensing-based ET estimation method is important for research on global change.

There are four types of remote sensing-based methods on ET estimation: i) surface energy balance (SEB) methods (Kustas and Norman, 1996; Su, 2002; Bastiaanssen et al., 2005; Overgaard et al., 2006; Allen et al., 2007); ii) methods that employ simplified process models such as the Penman–Monteith (P–M) equation (Monteith, 1965) and remote sensing data (Cleugh et al., 2007; Mu et al., 2007); iii) methods that employ empirical relationships between the vegetation index and ET, such as the triangle method and its derivates (Nemani and Running, 1989; Gillies et al., 1997; Nishida et al., 2003; Tang et al., 2009); and iv) methods that employ assimilation of remote sensing data into models (Olioso et al., 1999, 2005; Courault et al., 2005; Pan and Wood, 2006; Irmak and Kamble, 2009).

In the case of SEB methods, the main step is to estimate surface sensible heat flux, which is sensitive to the aerodynamic resistance of the canopy. However, canopy aerodynamic resistance is difficult to estimate accurately, because it requires knowledge of the wind field, planetary boundary information, and roughness length. The simplified P–M model, on the other hand, provides relatively robust estimation of ET, yet this method is limited by its

Received September 24, 2012; accepted October 8, 2012

E-mail: shirunhe@gmail.com

need for data on meteorology forcing, aerodynamic resistance and surface resistance. Following the ideas of Nemani and Running (1989), the empirical triangle method uses the slope of a scatterplot of a vegetation index (*VI*) against surface temperature (T_s) as an approximation of surface resistance. However, this method requires a large number of pixels over a flat area with a wide range of soil moisture and fractional vegetation cover to ensure that the dry and wet edge exists in the *VI*–T_s triangle space (Li et al., 2009).

In view of the drawbacks of the above four methods, researchers are investigating approaches that apply remote sensing data to extrapolate ET measured at flux towers to a regional scale. Nagler et al. (2005b) developed an empirical relationship to predict ET over large reaches of rivers in the western United States by combining the enhanced vegetation index (EVI), measured air temperature, and ET. The evaluation result had a coefficient of determination (R^2) value of 0.75 and root-mean-square error (*RMSE*) of 1.09 mm/d. Yang et al. (2006) used a support vector machine (SVM) to estimate ET over the continental United States. The SVM was trained with ET measurements taken at 25 AmeriFlux sites and satellite-derived land surface temperature (*LST*), EVI, land cover, and shortwave radiation (SWR). They showed that the SVM could reproduce the spatial and temporal variation of ET at a continental scale (R^2 = 0.75; *RMSE* = 0.66 mm/d). Lu and Zhuang (2010) combined remote sensing data, meteorology data, and flux-tower-measured ET to develop a continental ET estimation model using an artificial neural network (ANN). They first trained an ANN to predict the evapotranspiration fraction (EF) using ET measured at 28 AmeriFlux sites, five remote sensing derived variables (*LST*, Normalized Difference Vegetation Index(*NDVI*), normalized difference water index, leaf area index, and photosynthetically active radiation) and two ground-measured variables — air temperature and wind velocity — during 2003–2005. ET was then calculated by multiplying net radiation flux and the EF estimated by the ANN. Finally they estimated and evaluated ET at 24 AmeriFlux sites during 2006. The R^2 value in comparison of the estimated and measured ET varied from 0.53 to 0.86.

In this study, an ANN based on remote sensing data and flux measurements was established to estimate ET. There are three main differences from the method of Lu and Zhuang (2010). First, the neural network inputs are simplified to three remote sensing variables, *NDVI*, *LST,* and surface net radiation (R_n), in our model. Second, we trained the ANN to predict ET directly, instead of the EF, using remote sensing data. Finally, the five validation flux sites are not involved in the network training. This strategy is expected to provide a better and more objective validation of our new model.

2 Data and method

2.1 Data

2.1.1 Measurements at AmeriFlux sites

We acquired half-hourly latent heat flux (LE) data measured by eddy covariance method (with relative accuracy of 25% (Falge et al., 2001)) at 18 AmeriFlux sites. These sites covered eight vegetation types according to IGBP (International Geosphere–Biosphere Programme) classification system and were distributed across the continental United States (Table 1). To match the temporal interval of the remote sensing data, the half-hourly LE is averaged over eight days. The eight-day averaged LE is transformed to ET by dividing by the latent heat of vaporization for 1 mm water per m^2 (2.45×10^6 J) (Allen et al., 1998).

2.1.2 Remote sensing data

ET is controlled by many factors, including climate, plant biophysics, soil properties, and topography (Mu et al., 2007). In considering the availability of remote sensing data and the simplicity of our model, we selected *NDVI*, *LST,* and R_n (daily surface net radiation) as input variables for ET estimation.

We obtained the VIs, namely the EVI and NDVI (MYD13Q1, with 250 m resolution and 16-day composite interval) and LST (MYD11A2, with 1 km resolution and eight-day composite interval), from MODIS Land Product American Standard Code for Information Interchange (ASCII) subsets[1]. Previous researches indicate that the VI products have accuracy better than 0.03 (Gao et al., 2003). Additionally, error in the LST product is no more than 1 K. Each 16-day-composed VI product was divided into two eight-day VI products with no change in accuracy.

The R_n was calculated with the following equation.

$$R_n = R_{sw\downarrow} - R_{sw\uparrow} + R_{lw\downarrow} - R_{lw\uparrow}, \quad (1)$$

where, $R_{sw\uparrow}$ is surface upwelling shortwave radiation, $R_{sw\downarrow}$ is surface downwelling shortwave radiation, $R_{lw\uparrow}$ is surface upwelling longwave radiation and $R_{lw\downarrow}$is surface downwelling longwave radiation. These data are derived from NASA GEWEX-SRB (Global Energy and Water Cycle Experiment — Surface Radiation Budget project) Release 3.0 data sets[2] at 1° × 1° resolution. Comparing with the ground observation of the Baseline Surface Radiation Network, daily $R_{sw\downarrow}$ of the GEWEX-SRB product has a bias of –3.2 $W \cdot m^{-2}$ and *RMSE* of 35.7 $W \cdot m^{-2}$. The bias of daily $R_{lw\downarrow}$ is –0.5 $W \cdot m^{-2}$ and the *RMSE* is 21.8 $W \cdot m^{-2}$. The eight-day averaged R_n is derived from daily R_n values.

1) http://daac.ornl.gov/cgi-bin/MODIS/GR_col5_1/mod_viz.html
2) http://eosweb.larc.nasa.gov/PRODOCS/srb/table_srb.html

Table 1 Description of AmeriFlux sites used in this study

Site	Latitude	Longitude	Land cover	Time period	Citation
ARM Southern Great Plains	36.61	−97.49	GRS	2003–2006	Sims and Bradford (2001)
Atqasuk	**70.47**	**−157.41**	**GRS**	**2003–2006**	
Blodgett Forest	38.90	−120.63	ENF	2002–2006	Misson et al. (2007)
Bondville	**40.01**	**−88.29**	**CRP**	**2002–2006**	**Hollinger et al. (2005)**
Fort Peck	48.31	−105.10	GRS	2002–2006	
Goodwin Creek	34.25	−89.97	CRP	2002–2006	
Harvard_Forest	42.53	−72.19	MF	2002–2006	Urbanski et al. (2007)
Ivotuk	68.49	−155.75	OSH	2003–2006	
Kennedy Space Center (scrub oak)	28.61	−80.67	EBF	2002–2006	Dore et al. (2003)
Mead-irrigated maize-soybean rotation	41.16	−96.47	CRP	2002–2006	Verma et al. (2005)
Mead-rainfed maize-soybean rotation	41.18	−96.44	CRP	2002–2006	Verma et al. (2005)
Metolius-Intermediate	44.45	−121.56	ENF	2002–2006	Verma et al. (2005)
Morgan Monroe State Forest	**39.32**	**−86.41**	**DBF**	**2002–2003 2005–2006**	
Niwot Ridge	**40.03**	**−105.55**	**ENF**	**2002–2006**	
Tonzi Ranch	**38.43**	**−120.97**	**WSV**	**2002–2006**	**Ma et al. (2007)**
Vaira Ranch	38.41	−120.95	WSV	2002–2006	Xu and Baldocchi (2004)
Willow Creek	45.81	−90.08	DBF	2002–2006	Mackay et al. (2007)
Wind River Crane	45.82	−121.95	ENF	2002–2006	Chen et al. (2004)

Notes: CRP, cropland; DBF, broadleaf forest; EBF, deciduous evergreen broadleaf forest; ENF, evergreen needleleaf forest; GRS, grassland; MF, mixed forest; OSH, open shrubland; WSV, woody savanna. Sites in bold font are selected to validate ET estimation model established in this study

2.2 Method

2.2.1 ANN description

An ANN is a computational system that simulates the learning mechanism of a biologic neural network. The fundamental processing element of an ANN is the neuron. An artificial neuron receives inputs from other neurons or external sources and sums them after multiplying them with a weight. The result is then passed to a transfer function which transforms the input signal and delivers it to the next neuron. The way neurons are interconnected in a network is referred to as the network structure. A network in which signals propagate forward from an input to an output layer is called a feed-forward network. The multilayer perceptron (MLP), the most common and widely used feed-forward network, is applied in this study. The first layer of the MLP is the input layer, which consists of input variables of our model. And the last layer is the output layer, which consists of output results. Layers between input and output layers are hidden layers. All the neurons in a layer are connected with all neurons in the previous layer (except in the case of the input layer) and the next layer (except in the case of the output layer).

The neural network needs to be trained after defining its structure. We select the back-propagation algorithm, which was developed by Rumelhart et al. (1986), to adjust the weight in the MLP network to achieve the best fit with the input data. The common training process for the back-propagation algorithm is as follows.

1) Introduce the training data into the network and obtain the network outputs;

2) Compare the network outputs with observation data to obtain the total error;

3) Back-propagate the total error through the network to obtain the error of each neuron in the hidden layer and adjust the weight of the neuron to obtain the minimum error;

4) If either the previously defined goal of error or maximum number of training cycles is not reached, start the next training cycle.

Further detail on the MLP feed-forward network and back-propagation algorithm may be found in Haykin (1994).

2.2.2 Training and validation of the ANN model

The structure of the final ANN model that was used to estimate ET is shown in Fig. 1. The inputs of the ANN model are three remote sensing data (*NDVI*, *LST,* and R_n); there are two hidden layers, each with a tangent sigmoid transfer function ‘tansig’; the output is the ET value, with a linear transfer function ‘purelin’. Here ‘tansig’ transfer function is defined as

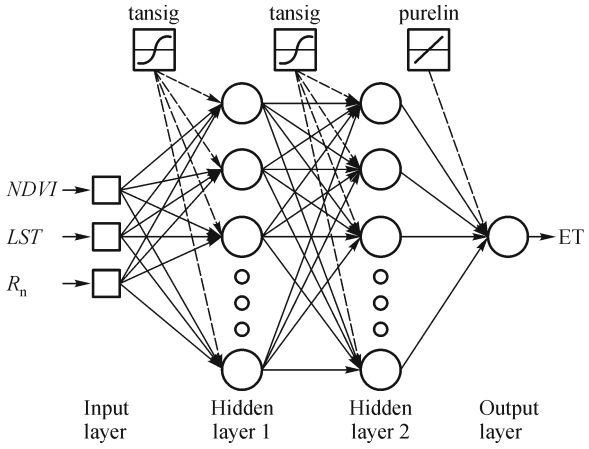

Fig. 1 The structure of the ANN model used in our study. 'tansig' represents tangent sigmoid transfer function; 'purelin' represents linear transfer function

$$\text{tansig}(x) = 2/\left(1+\exp(-2x)\right)-1, \qquad (2)$$

where x represents the corresponding input. To prevent the ANN model from being trapped in a local minimum error during training, all input and output variables of the network are normalized between 0 and 1.We divided 18 AmeriFlux sites into two groups. Thirteen sites were used for ANN training and five sites for validation. Because of the limited vegetation types covered by the 18 AmeriFlux sites, three vegetation types in the training group are not covered by validation sites.

3 Results

3.1 Validation for all five validation sites

The ANN model was applied to predict ET during 2002 and 2006 at the five validation sites which are not used for model training. The overall validation R^2 is 0.77 and the *RMSE* is 0.62 mm/d (Fig. 2). This result indicates that the estimated ET shows a good linear relationship with the measured ET and the error is controlled at a relatively low level. As shown in Fig. 3, the residuals (measured ET minus estimated ET) at the five validation sites are randomly distributed and mostly limited at ±2 mm/d.

3.2 Validation for each validation site

The estimation performance of the ANN at each validation site is presented in Table 2 and the five plots in Fig. 4. Four of the five validation sites, Morgan Monroe State Forest, Niwot Ridge, Tonzi Ranch, and Bondville have R^2 values above 0.70, while R^2 for Atqasuk is a bit lower of 0.59. In terms of the *RMSE*, Niwot Ridge has the highest estimation error of about 0.77 mm/d, and Tonzi Ranch has the lowest

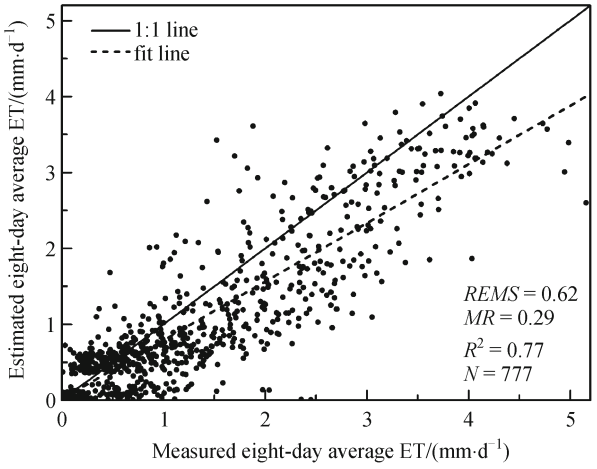

Fig. 2 Scatterplot of overall ANN-estimated ET and measured ET at five validation sites. The solid line represents a 1:1 relationship and the dashed line represents a linear fit

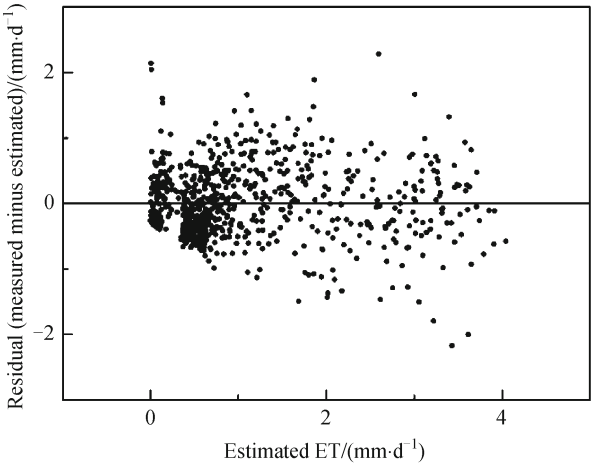

Fig. 3 Scatterplot of overall residuals (measured ET minus estimated ET) at five validation sites

estimation error of 0.49 mm/d. Niwot Ridge also has the largest bias of 0.68 mm/d.

Figure 4 shows the time series of ANN-estimated ET and flux-tower-measured ET. There are significant differences between estimated ET and measured ET at several validation sites. In the case of the Morgan Monroe State Forest, the ET was underestimated in the summer of 2002 and 2004. This may be due to the saturation of the satellite-derived NDVI in that season. The ANN underestimated ET for most of 2002 and 2006 at Niwot Ridge. However, the linear relationship between measured and estimated ET is good (R^2 = 0.81), and thus there may be systematic error existing in the ET measurements at this site. In the case of Atqasuk, there were some high ET measurements in the spring and winter of 2003 and 2004. Since this site is located in Alaska, where the temperature is extremely low in winter and spring, these high ET values may be caused

Table 2 Validation results of the ANN model with inputs of *NDVI*, *LST* and R_n

Site name	Land cover	R^2	*RMSE*	*MR*/(mm·d^{-1})
Morgan Monroe State Forest	DBF	0.84	0.59	−0.02
Niwot Ridge	ENF	0.81	0.77	0.68
Tonzi Ranch	WSV	0.70	0.49	0.19
Atqasuk	GRS	0.59	0.57	0.29
Bondville	CRP	0.78	0.63	0.26

Notes: CRP, cropland; DBF, broadleaf forest; ENF, evergreen needleleaf forest; GRS, grassland; WSV, woody savanna

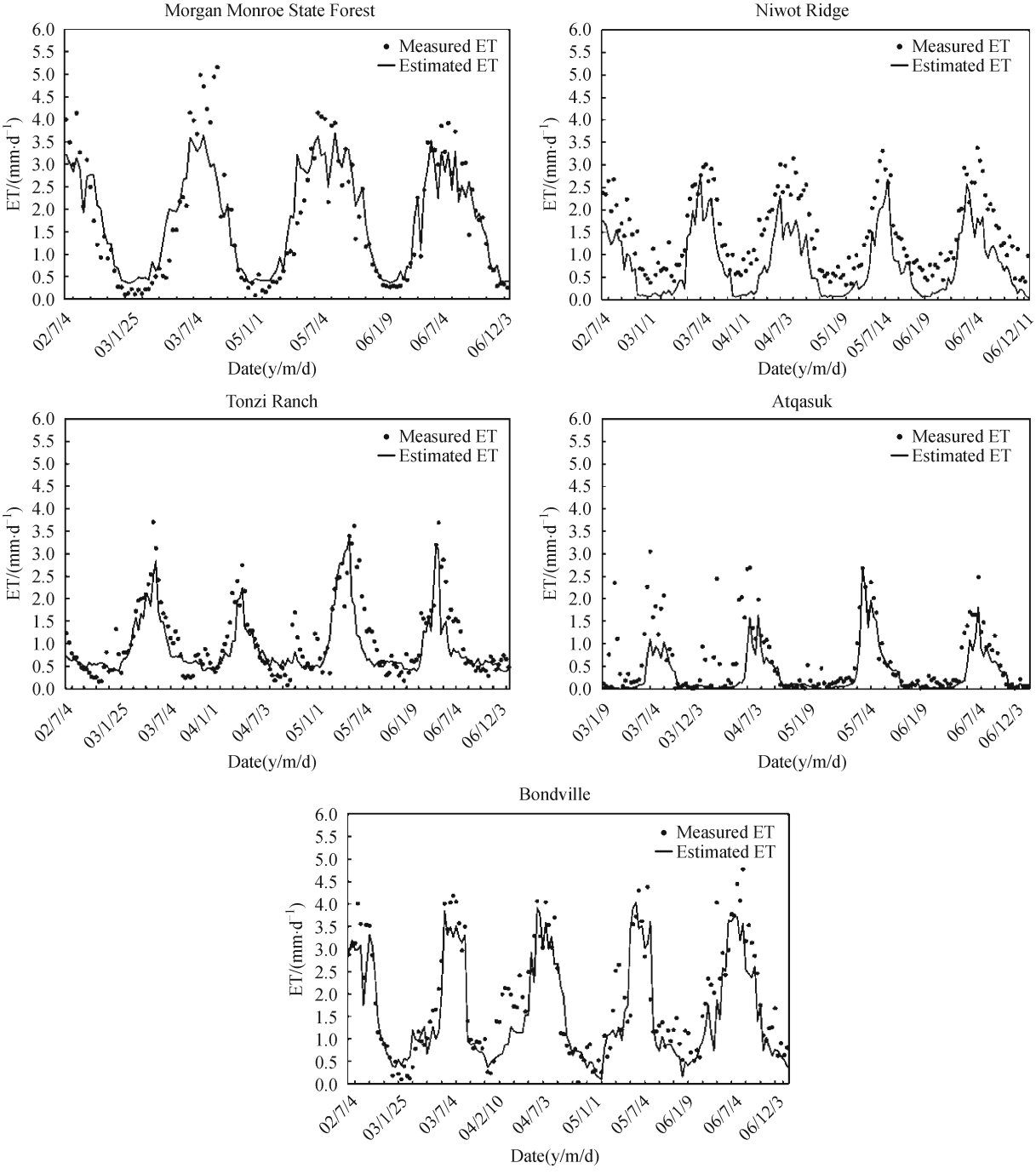

Fig. 4 Time series of ANN-estimated ET and measured ET at each validation site. The solid line represents ANN-estimated ET and the dots represent the measured ET

by measurement error. Despite these uncertainties in ET estimation, the ANN model generally captured the seasonal and interannual variation of the actual ET.

4 Discussion

4.1 Accuracy comparison between the ANN model and a simplified P–M model

Mu et al. (2011) developed an improved ET algorithm based on a simplified P–M model and produced the latest global ET product. Comparing validation results calculated by Mu's algorithm (Table 3) with those by our approach (Table 2) at the five validation sites, we found that the *RMSE* of our approach is smaller except for Atqasuk site. If we simply assume that the coefficient of determination (R^2) is the square of correlation coefficient (R), then the coefficient of determination (R^2) in our approach is higher than latest global ET product. Therefore, our approach showed a favorable accuracy with fewer inputs and calculations.

4.2 Surrogates for *NDVI* and R_n

Some researchers have used the MODIS EVI (Nagler et al., 2005a, 2005b; Yang et al., 2006) and SRB incoming SWR (Yang et al., 2006) to extrapolate flux-site-measured ET to a regional scale. To investigate the difference in estimation performance between using the *EVI* and *NDVI* and that between using the *SWR* and R_n, we trained and validated the ANN model after replacing the *NDVI* with the *EVI* and replacing R_n with $R_{sw\downarrow}$.

4.2.1 Replacing *NDVI* with *EVI*

Validation results of the ANN model with inputs of *EVI*, *LST,* and R_n are presented in Table 4. Comparing Table 2 and Fig. 4, we find that there was a slight decrease in overall estimation performance if we replace *NDVI* with *EVI*: R^2 decreased from 0.77 to 0.74 and the overall *RMSE* increased for only 0.01 mm/d, from 0.62 to 0.63. Different sites showed different effects. R^2 increased and RMSE decreased at Morgan Monroe State Forest, Niwot Ridge and Tonzi Ranch; R^2 remained the same, but the RMSE decreased at Bondville; and R^2 decreased and RMSE increased at Atqasuk. Considering the vegetation type for the five validation sites, we find that the EVI decreased the estimation performance for all vegetation types but grassland.

4.2.2 Replacing R_n with $R_{sw\downarrow}$

Validation results of the ANN model with inputs of *NDVI*, *LST,* and $R_{sw\downarrow}$ are presented in Table 5. Comparing these results with those introduced in Sect. 2.2, the overall R^2 for all validation sites decreased from 0.77 to 0.70 and the overall *RMSE* increased from 0.62 to 0.70 mm/d. The most significant decrease of R^2 was at the Bondville site, where R^2 decreased from 0.78 to 0.74 and *RMSE* increased from 0.63 to 0.77 mm/d. These results indicate that the use of $R_{sw\downarrow}$ instead of R_n in this ANN model causes more errors,

Table 3 Validation results of an ET estimation algorithm which based on a simplified P–M model and driven by MODIS data and Global Modeling and Assimilation Office (GAMO) meteorological reanalysis data (Mu et al., 2011)

Site name	Land cover	*R*	*RMSE*
Morgan Monroe State Forest	DBF	0.88	0.81
Niwot Ridge	ENF	0.68	1.00
Tonzi Ranch	WSV	0.78	0.68
Atqasuk	GRS	0.11	0.53
Bondville	CRP	0.78	1.03

Notes: CRP, cropland; DBF, broadleaf forest; EBF, deciduous evergreen broadleaf forest; ENF, evergreen needleleaf forest; GRS, grassland; WSV, woody savanna

Table 4 Validation results of the ANN model with inputs of *EVI*, *LST* and R_n

Site name	Land cover	R^2	*RMSE*	*MR*
All validation sites	–	0.74	0.65	0.29
Morgan Monroe State Forest	DBF	0.83	0.61	–0.06
Niwot Ridge	ENF	0.73	0.84	0.71
Tonzi Ranch	WSV	0.63	0.55	0.20
Atqasuk	GRS	0.70	0.52	0.28
Bondville	CRP	0.78	0.67	0.27

Notes: CRP, cropland; DBF, broadleaf forest; EBF, deciduous evergreen broadleaf forest; ENF, evergreen needleleaf forest; GRS, grassland; WSV, woody savanna

Table 5 Validation results of the ANN model with inputs of *NDVI*, *LST* and $R_{sw\downarrow}$

Site name	Land cover	R^2	*RMSE*	*MR*
All validation sites	–	0.70	0.70	0.32
Morgan Monroe State Forest	DBF	0.83	0.65	0.14
Niwot Ridge	ENF	0.80	0.88	0.75
Tonzi Ranch	WSV	0.58	0.55	0.08
Atqasuk	GRS	0.57	0.60	0.22
Bondville	CRP	0.74	0.77	0.43

Notes: CRP, cropland; DBF, broadleaf forest; ENF, evergreen needleleaf forest; GRS, grassland; WSV, woody savanna

especially for cropland regions.

4.3 Other factors influencing ANN model performance

The results in Sect. 3.2 indicate that the estimation performance of the ANN model differs for different vegetation types. In addition, its performance may also be affected by the following factors:

1) The uncertainty in ET measurements. ET observations used in this study were obtained by the eddy covariance method at fixed flux sites. Twine et al. (2000) and Wilson et al. (2002) found that energy imbalance problems existing in the method may overestimate energy by about 10–30%. Possible reasons include eddy covariance filtering the contribution of low frequency flux, advection, and the scale difference between the eddy covariance method and other energy measurement systems (Twine et al., 2000; Yi et al., 2000; Wilson et al., 2002).

2) The scale difference between the flux-site observation and remote sensing data. LST data have a spatial resolution of 1 km which covers much larger area than the footprint of the flux-site measurements. Nagler et al. (2005a) found that MODIS LST data at 1- and 5-km resolutions were too coarse to accurately measure the radiant surface temperature within a narrow riparian corridor. However, the spatial resolution of SRB R_n data are $1° \times 1°$, which is even more coarse. Therefore, net radiation at a flux site may differ from the SRB net radiation especially in an area with complex terrain and obvious heterogeneity.

5 Conclusions

An ANN model driven by remote sensing inputs of *NDVI*, *LST* and R_n is introduced to estimate ET in this study. Estimated ET is validated by site ET measurements. For all validation sites, the overall R^2 is 0.77 and the overall *RMSE* is 0.62 mm/d. There are differences in ET estimation performance for different vegetation types. The estimation accuracy is best for deciduous broadleaf forest followed by cropland, woody savannas, grassland, and evergreen needleleaf forest. These estimation results may be affected by uncertainty in the ET measurement as well as the inputs of *NDVI*, *LST* and R_n. Despite these uncertainties in ET estimation, the ANN model generally captured the seasonal and interannual variation in actual ET with favorable accuracy.

Except for grassland, the estimation performance for all vegetation types decreased after replacing the *NDVI* with the *EVI* in training the ANN. Estimation performances for all the five vegetation types were worse after R_n was replaced with $R_{sw\downarrow}$, and the greatest performance decrease was that for cropland. These results indicate that the use of the NDVI is better than that of the *EVI*, and that the use of R_n is better than that of $R_{sw\downarrow}$ in the ANN model to predict regional ET in this study.

Acknowledgements This work was supported by Shanghai Science and Technology Committee Program–Special for EXPO (No. 10DZ0581600), and the National Basic Research Program of China (No. 2010CB950902) , and the National Natural Science Foundation of China (Grant No. 41201358). The flux tower evapotranspiration measurement data were provided by AmeriFlux. We gratefully acknowledge all tower site principle investigators and their teams for providing the evapotranspiration data used in this study. MODIS Vegetation Indexes product and Land Surface Temperature product were obtained from Oak Ridge National Laboratory Distributed Active Archive Center. NASA GEWEX solar radiation data were obtained from the NASA Langley Research Center Atmospheric Science Data Center.

References

Allen R G, Pereira L S, Raes D, Smith M (1998). Crop evapotranspiration, guideline for computing water requirements. Irrigation Drainage Paper, No. 56. FAO, Rome, Italy

Allen R G, Tasumi M, Morse A, Trezza R, Wright J L, Bastiaanssen W, Kramber W, Lorite I, Robison C W (2007). Satellite-based energy balance for mapping evapotranspiration with internalized calibration (METRIC)—applications. J Irrig Drain Eng, 133(4): 395–406

Bastiaanssen W G, Noordman M, Pelgrum E J M, Davids G, Thoreson B P, Allen R G (2005). SEBAL model with remotely sensed data to improve water resources management under actual field conditions. J Irrig Drain Eng, 131(1): 85–93

Chen J, Kyaw T P U, Ustin S L, Suchanek T H, Bond B J, Brosofske K D, Falk M (2004). Net ecosystem exchanges of carbon, water, and energy in young and old-growth Douglas-Fir forests. Ecosystems (N. Y.), 7(5): 534–544

Cleugh H, Leuning A, Mu Q, Running S W (2007). Regional evaporation estimates from flux tower and MODIS satellite data. Remote Sens Environ, 106(3): 285–304

Courault D, Seguin B, Olioso A (2005). Review on estimation of evapotranspiration from remote sensing data: from empirical to numerical modeling approaches. Irrig Drain Syst, 19(3–4): 223–249

Dore S, Hymus G J, Johnson D P (2003). Climatic influences on net ecosystem CO_2 exchange during the transition from wintertime carbon source to springtime carbon sink in a high-elevation, subalpine forest. Oecologia, 146: 130–147

Falge E, Baldocchi D, Olson R J, Anthoni P, Aubinet M, Bernhofer C, Burba G, Ceulemans R, Clement R, Dolman H, Granier A, Gross P, Grünwald T, Hollinger D, Jensen N O, Katul G, Keronen P, Kowalski A, Ta Lai C, Law B E, Meyers T, Moncrieff J, Moors E, William Munger J, Pilegaard K, Rannik Ü, Rebmann C, Suyker A, Tenhunen J, Tu K, Verma S, Vesala T, Wilson K, Wofsy S (2001). Gap filling strategies for long term energy flux data sets. Agric Meteorol, 107(1): 71–77

Gao X, Huete A R, Didan K (2003). Multisensor comparisons and validation of MODIS vegetation indices at the semiarid Jornada Experimental Range. IEEE Trans Geosci Rem Sens, 41(10): 2368–2381

Gillies R R, Carlson T N, Cui J (1997). A verification of the 'triangle' method for obtaining surface soil water content and energy fluxes from remote measurements of the normalized difference vegetation index (NDVI) and surface e. Int J Remote Sens, 18(15): 3145–3166

Haykin S (1994). Neural Networks–A Comprehensive Foundation. New York: MacMillan College Publishing Company

Hollinger S E, Bernacchi C J, Meyers T P (2005). Carbon budget of mature no-till ecosystem in North Central Region of the United States. Agric Meteorol, 130(1–2): 59–69

Irmak A, Kamble B (2009). Evapotranspiration data assimilation with genetic algorithms and SWAP model for on-demand irrigation. Irrig Sci, 28(1): 101–112

Jung M, Reichstein M, Ciais P, Seneviratne S I, Sheffield J, Goulden M L, Bonan G, Cescatti A, Chen J, de Jeu R, Dolman A J, Eugster W, Gerten D, Gianelle D, Gobron N, Heinke J, Kimball J, Law B E, Montagnani L, Mu Q, Mueller B, Oleson K, Papale D, Richardson A D, Roupsard O, Running S, Tomelleri E, Viovy N, Weber U, Williams C, Wood E, Zaehle S, Zhang K (2010). Recent decline in the global land evapotranspiration trend due to limited moisture supply. Nature, 467: 951–954

Kustas W P, Norman J M (1996). Use of remote sensing for evapotranspiration monitoring over land surfaces. Hydrological Sciences Journal, 41(4): 495–516

Li Z L, Tang R, Wan Z, Bi Y, Zhou C, Tang B, Yan G, Zhang X (2009). A review of current methodologies for regional evapotranspiration estimation from remotely sensed data. Sensors, 9(5): 3801–3853

Lu X, Zhuang Q (2010). Evaluating evapotranspiration and water-use efficiency of terrestrial ecosystems in the conterminous United States using MODIS and AmeriFlux data. Remote Sens Environ, 114(9): 1924–1939

Ma S Y, Baldocchi D D, Xu L, Hehn T (2007). Inter-annual variability in carbon dioxide exchange of an oak/grass savanna and open grassland in California. Agric Meteorol, 147(3–4): 157–171

Mackay D S, Ewers B E, Cook B D, Davis K J (2007). Environmental drivers of evapotranspiration in a shrub wetland and an upland forest in northern Wisconsin. Water Resources Research, 43: W03442.1–W03442.14

Misson L, Baldocchi D D, Black T A, Blanken P D, Brunet Y, Curiel Yuste J, Dorsey J R, Falk M, Granier A, Irvine M R, Jarosz N, Lamaud E, Launiainen S, Law B E, Longdoz B, Loustau D, McKay M, Paw U K T, Vesala T, Vickers D, Wilson K B, Goldstein A H (2007). Partitioning forest carbon fluxes with overstory and understory eddy-covariance measurements: a synthesis based on FLUXNET data. Agric Meteorol, 144(1–2): 14–31

Monteith J L (1965). Evaporation and environment. Symp Soc Exp Biol, 19: 205–234

Mu Q, Heinsch F A, Zhao M, Running S W (2007). Development of a global evapotranspiration algorithm based on MODIS and global meteorology data. Remote Sens Environ, 111(4): 519–536

Mu Q, Zhao M, Running S W (2011). Improvements to a MODIS global terrestrial evapotranspiration algorithm. Remote Sens Environ, 115 (8): 1781–1800

Nagler P L, Cleverly J, Glenn E, Lampkin D, Huete A, Wan Z (2005a). Predicting riparian evapotranspiration from MODIS vegetation indices and meteorological data. Remote Sens Environ, 94(1): 17–30

Nagler P L, Scott R, Westenburg C, Cleverly J, Glenn E, Huete A (2005b). Evapotranspiration on western U.S. rivers estimated using the Enhanced Vegetation Index from MODIS and data from eddy covariance and Bowen ratio flux towers. Remote Sens Environ, 97 (3): 337–351

Nemani R R, Running S W (1989). Estimation of regional surface resistance to evapotranspiration from NDVI and thermal-IR AVHRR data. J Appl Meteorol, 28(4): 276–284

Nishida K, Nemani R R, Glassy J M, Running S W (2003). Development of an evapotranspiration index from aqua/MODIS for monitoring surface moisture status. IEEE Trans Geosci Rem Sens, 41(2): 493–501

Oki T, Kanae S (2006). Global hydrological cycles and world water resources. Science, 313(5790): 1068–1072

Olioso A, Chauki H, Courault D, Wigneron J P (1999). Estimation of evapotranspiration and photosynthesis by assimilation of remote sensing data into SVAT models. Remote Sens Environ, 68(3): 341–356

Olioso A, Inoue Y, Ortega-FARIAS S, Demarty J, Wigneron J P, Braud I, Jacob F, Lecharpentier P, OttlÉ C, Calvet J C, Brisson N (2005). Future directions for advanced evapotranspiration modeling: assimilation of remote sensing data into crop simulation models and SVAT models. Irrig Drain Syst, 19(3–4): 377–412

Overgaard J, Rosbjerg D, Butts M B (2006). Land-surface modeling in hydrological perspective—a review. Biogeosciences, 3(2): 229–241

Pan M, Wood E (2006). Data assimilation for estimating the terrestrial water budget using a constrained ensemble Kalman filter. J Hydrometeorol, 7(3): 534–547

Rumelhart D E, Hinton G E, Williams R J (1986). Learning representations by back-propagating errors. Nature, 323(6088): 533–536

Sims P L, Bradford J A (2001). Carbon dioxide fluxes in a southern plains prairie. Agric Meteorol, 109(2): 117–134

Su Z (2002). The surface energy balance system (SEBS) (for estimation of turbulent heat fluxes). Hydrol Earth Syst Sci, 6(1): 85–100

Tang Q, Peterson S, Cuenca R H, Hagimoto Y, Lettenmaier D P (2009). Satellite-based near real-time estimation of irrigated crop water consumption. J Geophys Res, 114(D5): D05114

Twine T E, Kustas W P, Norman J M, Cook D R, Houser P R, Meyers T P, Prueger J H, Starks P J, Wesely M L (2000). Correcting eddy-covariance flux underestimates over a grassland. Agric Meteorol, 103 (3): 279–300

Urbanski S, Barford C, Wofsy S, Kucharik C, Pyle E, Budney J, McKain K, Fitzjarrald D, Czikowsky M, Munger J W (2007). Factors controlling CO_2 exchange on timescales from hourly to decadal at Harvard Forest. J Geophys Res, 112(G2): G02020

Verma S B, Dobermann A, Cassman K G, Walters D T, Knops J M, Arkebauer T J, Suyker A E, Burba G G, Amos B, Yang H, (2005). Annual carbon dioxide exchange in irrigated and rainfed maize-based agroecosystems. Agricultural and Forest Meteorology, 131(1–2): 77–96

Wilson K, Goldstein A, Falge E, Aubinet M, Baldocchi D, Berbigier P, Bernhofer C, Ceulemans R, Dolman H, Field C, Grelle A, Ibrom A, Law B E, Kowalski A, Meyers T, Moncrieff J, Monson R, Oechel W, Tenhunen J, Valentini R, Verma S (2002). Energy balance closure at FLUXNET sites. Agric Meteorol, 113(1–4): 223–243

Xu L K, Baldocchi D D (2004). Seasonal variation in carbon dioxide exchange over a Mediterranean annual grassland in California. Agric Meteorol, 123(1–2): 79–96

Yang F, White M, Michaelis A, Ichii K, Hashimoto H, Votava P, Zhu A X, Nemani R R (2006). Prediction of continental-scale evapotranspiration by combining MODIS and Ameriflux data through support vector machine. IEEE Trans Geosci Rem Sens, 44(11): 3452–3461

Yi C, Davis K J, Bakwin P S, Berger B W, Marr L C (2000). Influence of advection on measurements of the net ecosystem-atmosphere exchange of CO_2 from a very tall tower. Journal of Geography Research, 105: 9991–9999

AUTHOR BIOGRAPHIES

Zhuoqi Chen obtained his bachelor degree in 2003 from Beijing Normal University, China and Ph.D. in Cartography and Geographic Information System from Institute of Geographic Sciences and Natural Resources Research, Chinese Academy of Sciences in 2009. In 2009, he began to work as a Junior Researcher at College of Global Change and Earth System Science, Beijing Normal University. His research interest include: remote sensing applications in ecological model and hydrometeorology. Dr. Chen published 4 papers as first author or corresponding author. E-mail: chenzq@bnu.edu.cn

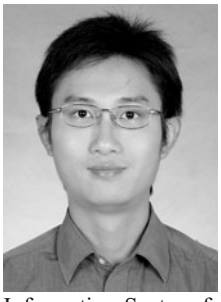

Runhe Shi is an Associate Professor in the Department of Geography at East China Normal University, China. He is working at the Key Laboratory of Geographic Information Science, Ministry of Education, China, and serves as an Assistant Director. He obtained his B.S. in Geography from East China Normal University in 2001 and Ph.D. in Cartography and Geographic Information System from the Institute of Geographic Sciences and Natural Resources Research, Chinese Academy of Sciences in 2006. His primary area of research is quantitative remote sensing including retrieval of plant biochemistry, greenhouse gases and particulate matters in the atmosphere. He has authored more than 50 refereed journal articles and conference papers. He is also the holder of two patents about data processing of remote sensing images. E-mail: shirunhe@gmail.com

Shupeng Zhang earned his Ph.D. in applied mathematics from Beijing Normal University, China in 2010. He has been working as a Junior Researcher for the college of global change and earth system science of Beijing Normal University since July 2010. His research fields focus on numerical solutions of partial differential equations, numerical simulations of fluids, atmospheric models and data assimilation. E-mail: spzhang@bnu.edu.cn